Supplementary Information (SI) for Materials Horizons.
This journal is © The Royal Society of Chemistry 2026

Supporting Information

Multi-state electromagnetic phase modulations in $NiCo_2O_4$ through cation disorder and hydrogenation

*Xuanchi Zhou [1, 2]† *, Xiaohui Yao [1]†, Shuang Li [1], Xiaomei Qiao [1], Jiahui Ji [1], Guowei Zhou [1, 2]*, Huihui Ji [1, 2], Xiaohong Xu [1, 2] **

[1] Key Laboratory of Magnetic Molecules and Magnetic Information Materials of Ministry of Education & School of Chemistry and Materials Science, Shanxi Normal University, Taiyuan, 030031, China

[2] Research Institute of Materials Science, Shanxi Key Laboratory of Advanced Magnetic Materials and Devices, Shanxi Normal University, Taiyuan 030031, China

*Authors to whom correspondence should be addressed: *xuanchizhou@sxnu.edu.cn (X. Zhou)*, *zhougw@sxnu.edu.cn (G. Zhou)*, and *xuxh@sxnu.edu.cn (X. Xu)*.

† X. Zhou, and X. Yao contributed equally to this work.

This file includes:

Supplementary Figures 1-16 and Supplementary References.

Contents

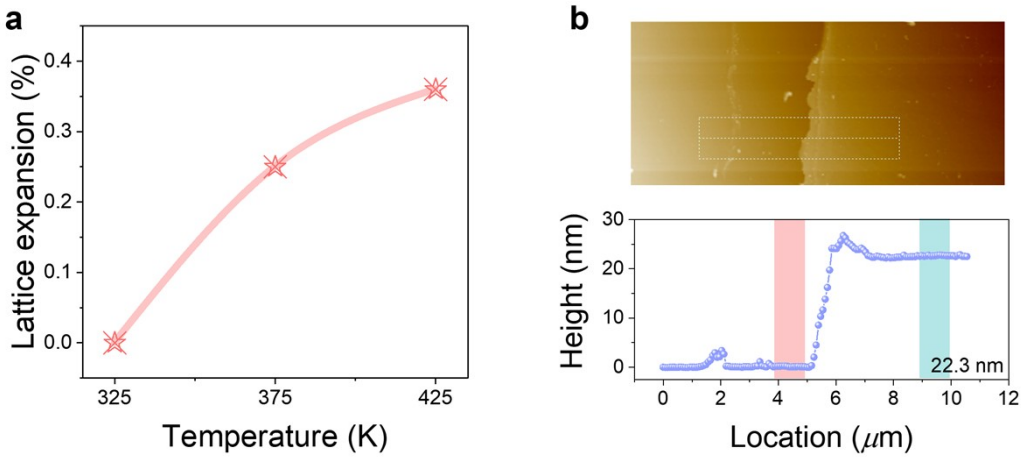

Supplementary Figure 1. a, *Out-of-plane* lattice expansion of NCO films as a function of deposition temperature ($T_{sub.}$). **b,** Atomic force microscope (AFM) images for as-grown 22 nm-thick NCO/MAO (001) heterostructure. Elevated growth temperatures promote cation disorder and the formation of oxygen vacancies, which cause *out-of-plane* lattice expansion and a corresponding low angle shift in the XRD spectra. Concurrently, the NCO films thickness is estimated to be around 22.3 nm using AFM techniques.

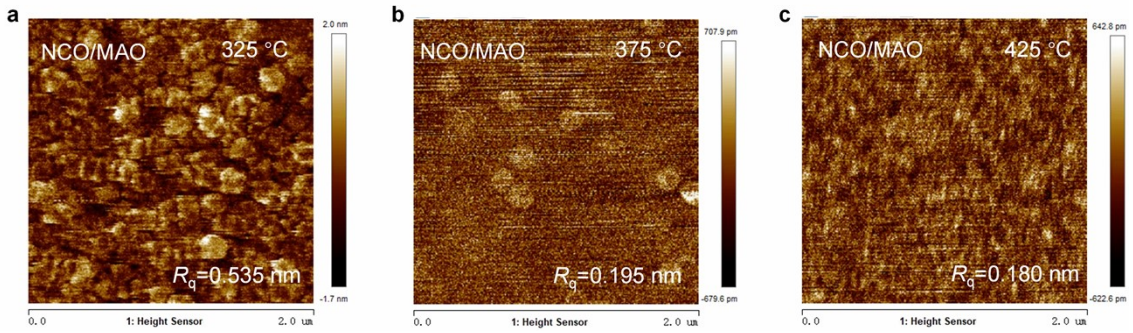

Supplementary Figure 2. Atomic force microscope (AFM) images for as-grown NCO/MAO heterostructure at different growth temperature. The as-grown NCO/MAO films exhibit atomically smooth surfaces, as quantified by AFM with a root-mean-square roughness (R_q) of less than 0.5 nm. Moreover, the surface smoothness of the film improves significantly with increasing growth temperature, a phenomenon attributed to the temperature-dependent plasma dynamics in the PLD process. A higher substrate temperature provides additional energy to the plasma plume, which accelerates its propagation toward the substrate. The arriving adatoms thereby gain higher surface mobility, facilitating more efficient diffusion and incorporation into low-energy lattice sites. This process promotes two-dimensional layer-by-layer growth and ultimately yields a smoother, denser film surface.[1]

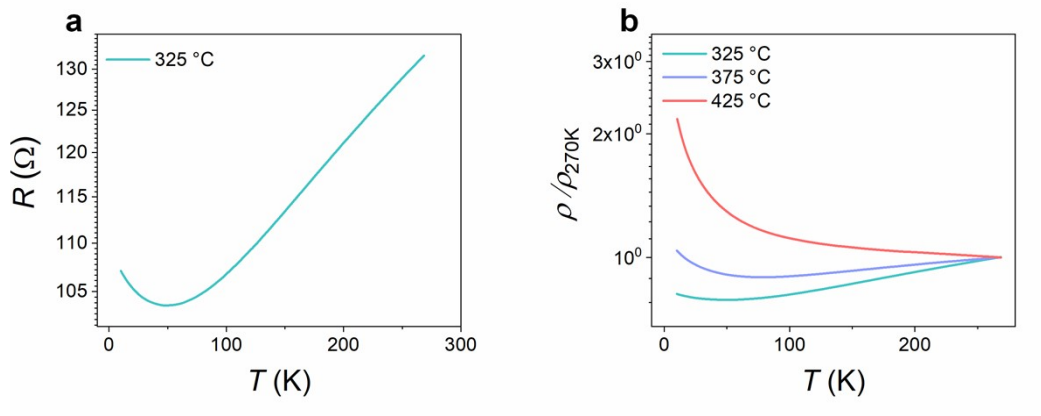

Supplementary Figure 3. a. Temperature dependence of resistance (*R*-*T*) for an NCO film deposited at 325 °C. **b.** Temperature-dependent normalized resistivity (ρ/ρ_{270K}) for NCO films deposited at different substrate temperatures. It is found that the material resistivity for NCO/MAO heterostructure grown at 325 °C showcase a rising tendency with the temperature (e.g., dR/dT >0), characteristic of typical metallic conductivity. Nevertheless, down to around 50 K, below which a resistivity upturn is observed, primarily attributed to the enhanced electron-electron interactions in low-temperature region.[2] Remarkably, the electronic phase transition from metal to semiconductor state is achieved for NCO film via elevating the growth temperature to 425 °C.

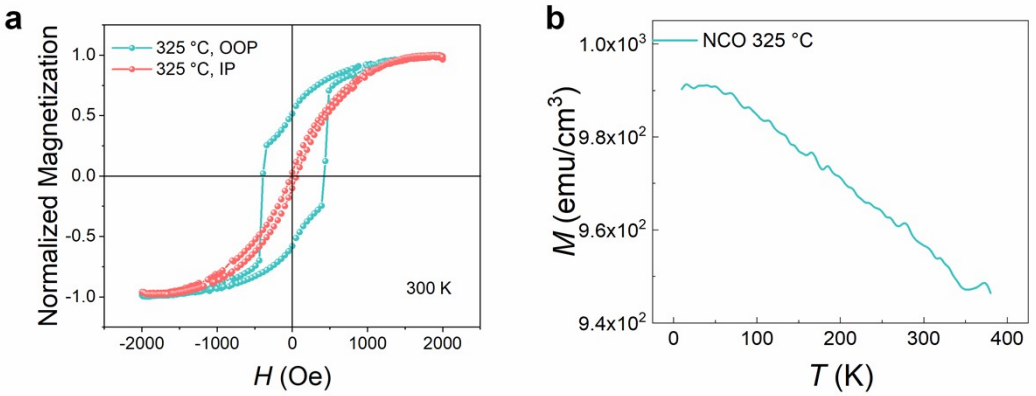

Supplementary Figure 4. a. The magnetization hysteresis (*M*-*H*) loops compared for NCO films deposited at 325 °C along the OOP and IP directions at 300 K. **b.** Temperature-dependent magnetization (*M*-*T*) for as-grown NCO/MAO heterostructure at 325 °C, measured from 10 K to 380 K. The grown NCO film at 325 °C exhibits a robust PMA, meanwhile, magnetic measurements reveal a Curie temperature (T_c) above 380 K for the NCO film deposited at 325 °C, consistent with the bulk value.

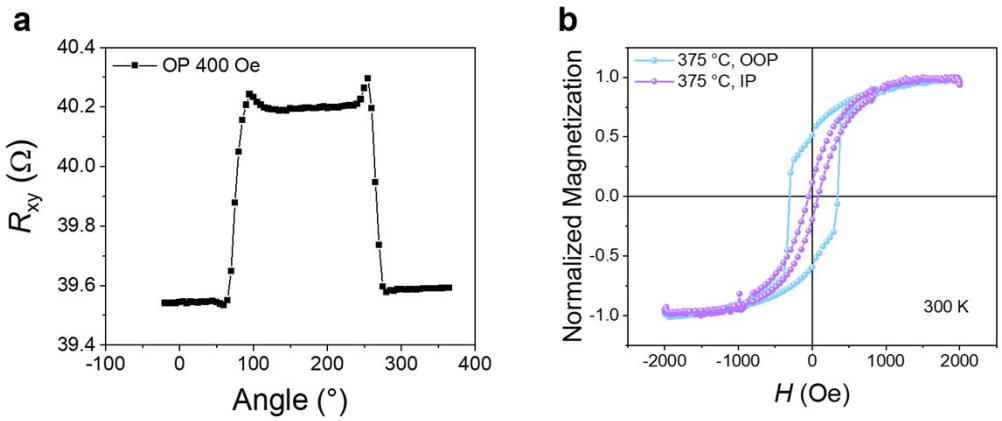

Supplementary Figure 5. a, Angle dependence of the Hall resistance under the magnetic fields of 400 Oe. **b,** Dependence of OOP and IP magnetization on the magnetic field at 300 K for NCO films deposited at 375 °C. The measurement results from angle dependence of the Hall resistance demonstrate an *out-of-plane-oriented* easy magnetic axis,[3] which is further confirmed by comparing the *M-H* loops of the NCO film grown at 375 °C along the *out-of-plane* and *in-plane* directions.

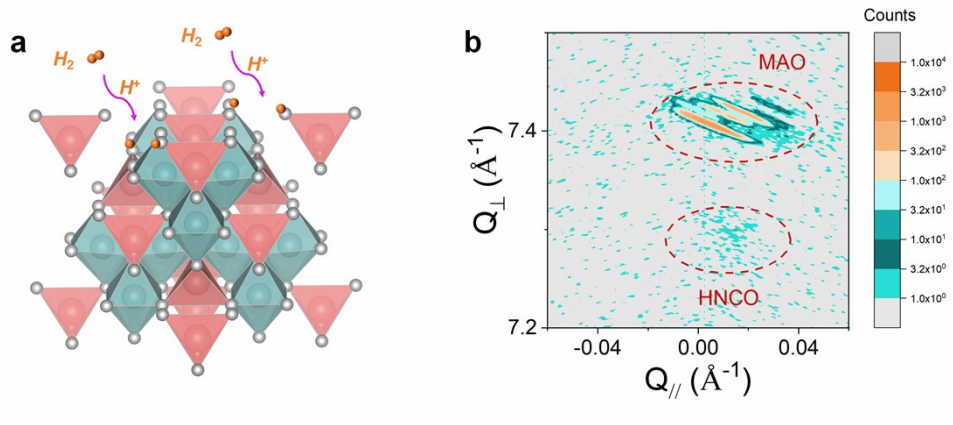

Supplementary Figure 6. a, Schematic of hydrogenation process using Pt-assisted hydrogen spillover strategy. **b,** Reciprocal space mapping (RSM) for hydrogenated NCO/MAO heterostructure. The catalytic function of Pt markedly reduces the energy barrier for H_2 dissociation into H^+ and electrons at the three-phase interface, which in turn facilitates the efficient insertion of hydrogen ions into the lattice. After hydrogenation, the identical *in-plane* scattering vector (e.g., $Q_{\parallel}$) between the NCO film and the MAO substrate confirms the epitaxial growth of the NCO/MAO (001) heterostructure, a shift in the *out-of-plane* vector (e.g., $Q_{\perp}$) is observed compared to the pristine film, demonstrating lattice expansion along the cross-plane direction due to hydrogen ion insertion. The peak intensity associated with the NCO film in the RSM spectra is extensively depressed through hydrogenation.

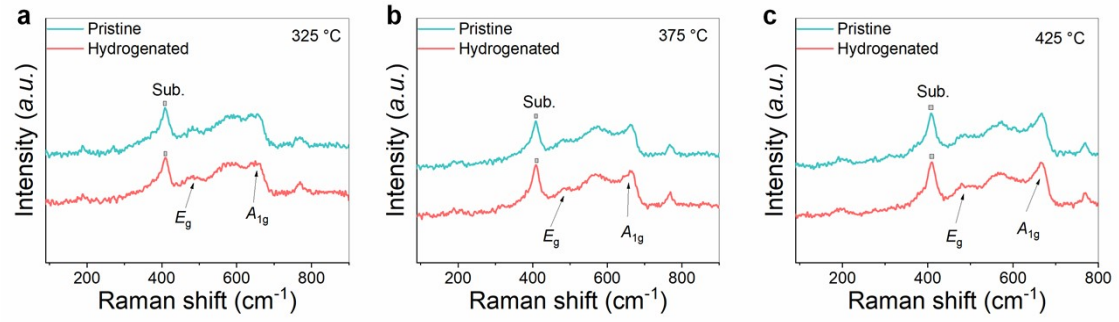

Supplementary Figure 7. Raman spectra comparison between pristine and hydrogenated NCO films deposited at **a,** 325 °C, **b,** 375 °C and **c,** 425 °C. The E_g mode corresponds to the vibration of oxygen atoms perpendicular to the metal-oxygen bonds and is typically associated with the symmetry of octahedral sites (O_h). In contrast, the A_{1g} mode arises from the symmetric stretching vibration of oxygen atoms along the metal-oxygen bonds and is commonly related to the symmetry of tetrahedral sites (T_d).[4] The characteristic phonon modes of the parent NCO phase are retained after hydrogenation, confirming that the primary lattice framework remains intact, consistent with a topotactic phase transformation.

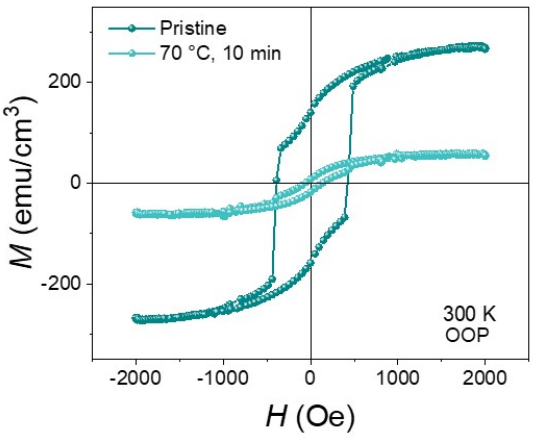

Supplementary Figure 8. *M-H* loops measured at 300 K for pristine and hydrogenated NCO films deposited at 325 °C along the *out-of-plane* direction. The PMA of pristine NCO is suppressed through hydrogenation, accompanied by the reduction in the saturation magnetization (M_s) and coercive field (H_c).

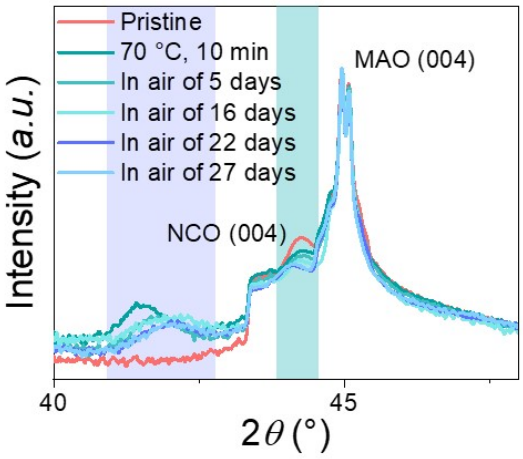

Supplementary Figure 9. XRD patterns compared for NCO/MAO heterostructure upon hydrogenation and dehydrogenation. The intermediate hydrogenated phase exhibits lower stability compared to the fully hydrogenated state (formed at 100 °C for 1 h). Furthermore, its characteristic diffraction peak gradually reverts toward the pristine state after 16 days of ambient exposure, further underscoring its metastable nature.

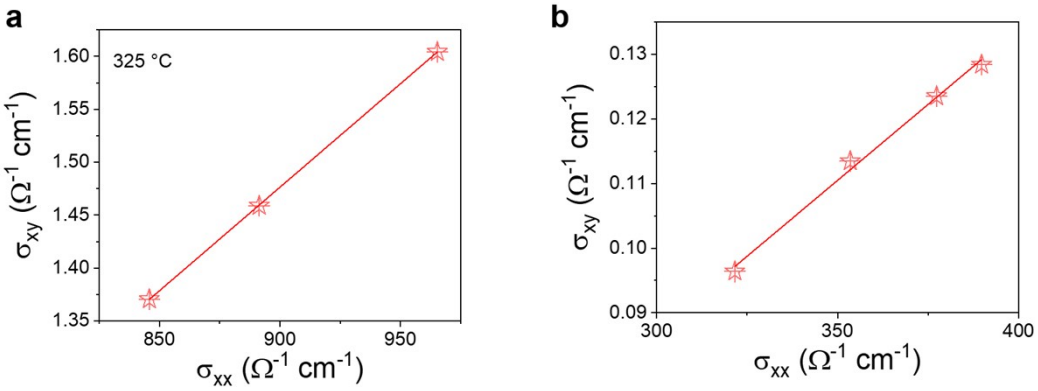

Supplementary Figure 10. Scaling relation between anomalous Hall conductivity (σ_{xy}) and longitudinal conductivity (σ_{xx}) for **a,** pristine and **b,** hydrogenated NCO films deposited at 325 °C. The Scaling relation between σ_{xy} and σ_{xx} can be described by using $\sigma_{xy} = A\sigma_{xx}^{1.6}$+B, with the A representing the extrinsic contribution (primarily from skew scattering and side jump) and the B corresponding to the intrinsic Berry curvature contribution.[5, 6]

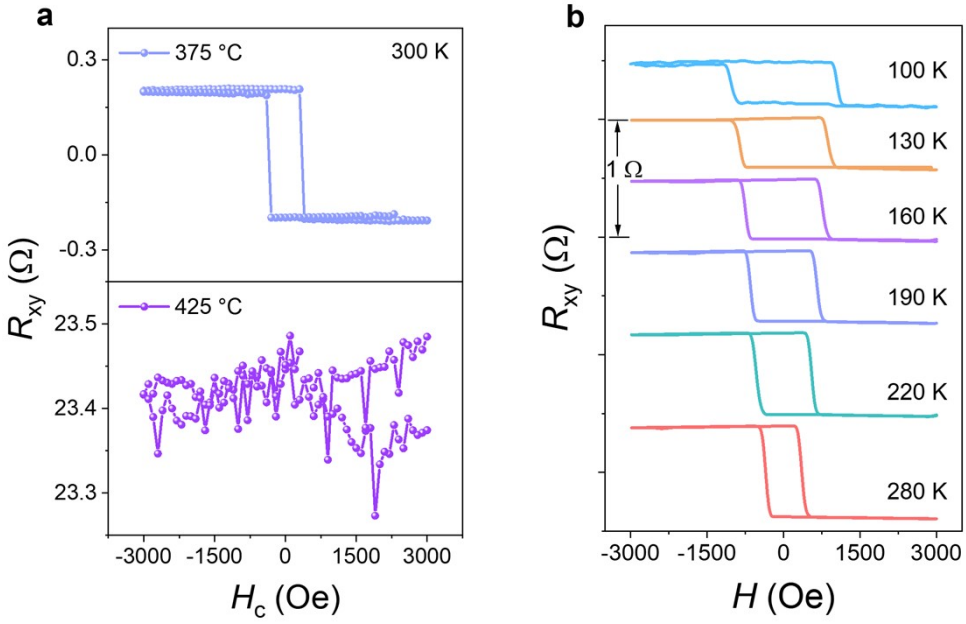

Supplementary Figure 11. Evolution of anomalous Hall resistivity (AHE) with substrate growth temperature measured at 300 K. **b,** Temperature-dependent AHE loops for NCO film deposited at 375 °C. As the growth temperature increases, it drives a significant enhancement of disorder, which in turn leads to the gradual suppression of the anomalous Hall effect (AHE).

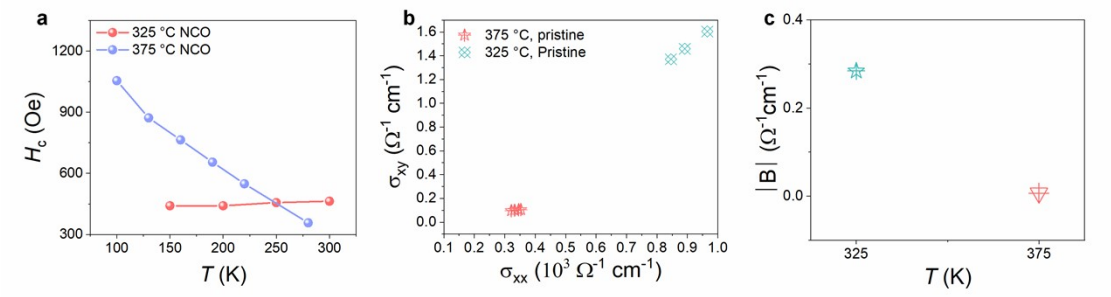

Supplementary Figure 12. a, Temperature-dependence of Coercive Field (H_c) for NCO pristine through improve growth temperature introduce cation disorder. **b,** Modulation of the intrinsic anomalous hall contribution by increased the growth temperature. **c,** Scaling between longitudinal and hall conductivity in NCO Films tuned by growth temperature. Apart from the suppression of Hall resistance (R_{xy}) due to cation disorder induced by elevated growth temperature, the coercive field (H_c) extracted from anomalous Hall effect (AHE) loops exhibits an exponential increase as temperature decreases. This distinct temperature dependence of H_c in disorder-enhanced NCO films likely originates from enhanced domain-wall pinning caused by cation disorder introduced through high temperature growth. Following an approach similar to that used for hydrogenation, a scaling analysis was performed by correlating the anomalous Hall conductivity with the longitudinal conductivity via the relation $\sigma_{xy} = A\sigma_{xx}^{1.6}$+B. The AHE is determined by intrinsic band intrinsic contribution (coefficient B) and scattering-dependent extrinsic contribution arising from the skew scattering and side jump ($A\sigma_{xx}^{1.6}$). Fitting based on this scaling relation reveals that the magnitude of coefficient B, associated with the intrinsic Berry curvature, decreases significantly with increasing disorder. This suggests a relative enhancement of the scattering-dominated extrinsic mechanism, signaling a transition of the system toward a disorder-dominated scattering regime. This shift mirrors the effect of cation disorder introduced in pristine NCO by raising the growth temperature, further confirming that disorder induced by elevated growth temperature and disorder introduced via hydrogenation share a similar underlying mechanism-both enhance domain-wall pinning and alter carrier scattering pathways, thereby modulating magneto transport properties.[1, 7]

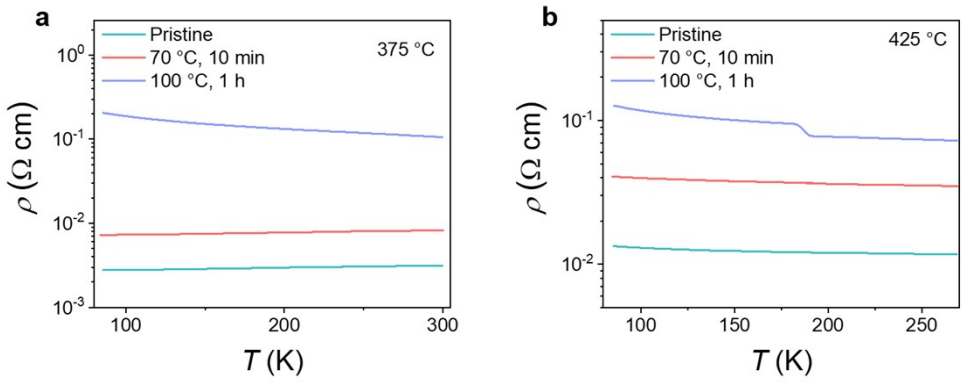

Supplementary Figure 13. a, Temperature-dependent resistivity (ρ-T) curves for pristine and hydrogenated NCO films grown at 375 °C. **b,** ρ-T curves for pristine and hydrogenated NCO films grown at 425 °C. The smaller modulation in resistivity upon hydrogenation indicates that higher cation disorder originating from elevated temperature growth partially suppresses the proton-induced electronic phase evolution. In NCO films with higher cation disorder, hydrogen incorporation exerts a weaker influence on electrical transport than in more ordered films. This suggests that pre-existing structural and electronic disorder kinetically hinders proton-driven carrier localization, highlighting the role of cation disorder as a tuning parameter for hydrogen-related phase transitions.

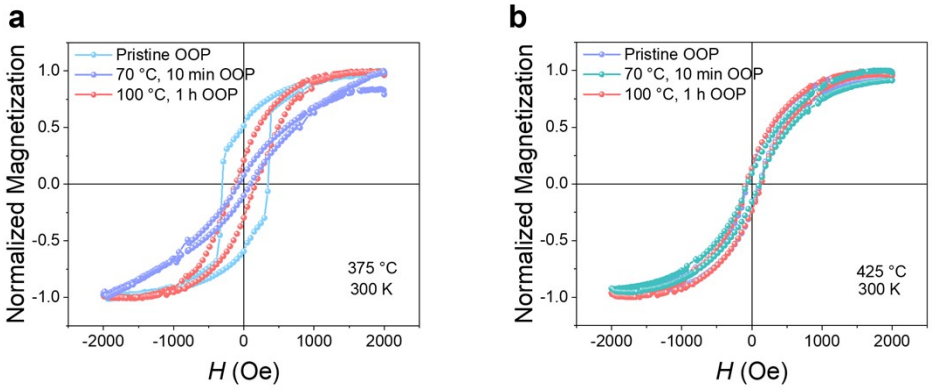

Supplementary Figure 14. The normalized magnetization hysteresis (*M-H*) loops compared for pristine and hydrogenated NCO films deposited at **a,** 375 °C and **b,** 425 °C along the OOP and IP directions at 300 K. While hydrogenation effectively tunes the PMA in NCO with low disorder, it shows negligible effect in highly disordered systems. This occurs as the magnetic ground state is already profoundly modified by cation disorder, which leaves insufficient phase space for additional modulation by hydrogen ions.

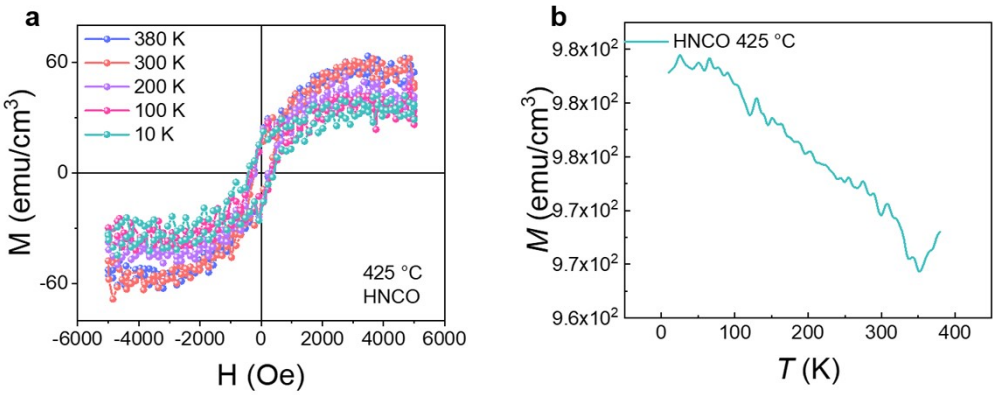

Supplementary Figure 15. a, Temperature-dependent *out-of-plane M-H* loops for NCO deposited at 425 °C, measured from 10 K to 380 K. **b,** Temperature-dependent magnetization (*M-T*) for as-grown NCO/MAO heterostructure at 425 °C, measured from 10 K to 380 K.

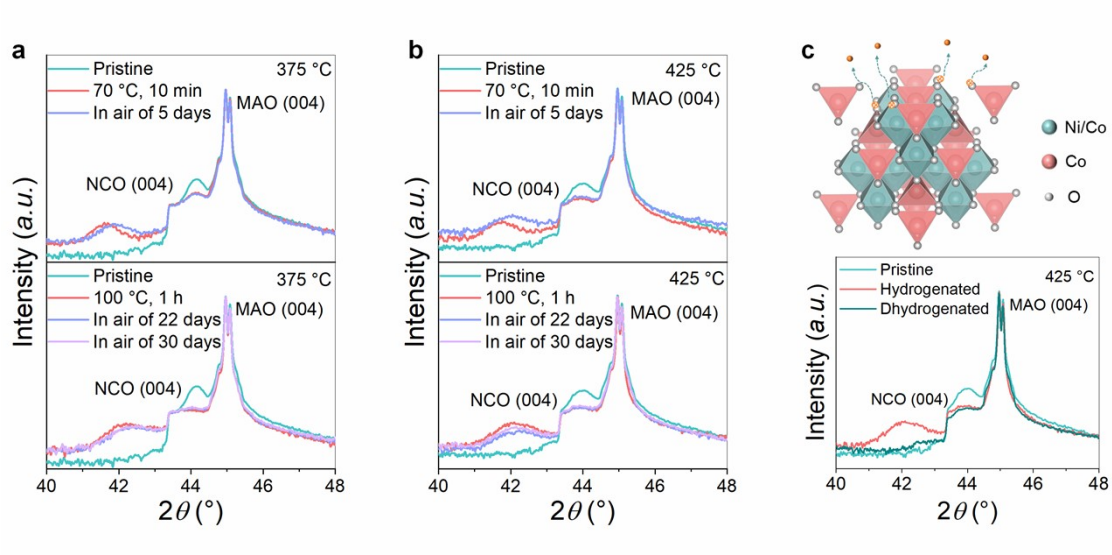

Supplementary Figure 16. Evolution of XRD patterns with hydrogenation for NCO films grown at **a,** 375 °C and **b,** 425 °C. **c,** XRD patterns compared for NCO/MAO heterostructure upon hydrogenation and dehydrogenation. When exposed to air, the intermediate hydrogenated NCO film exhibits a gradual recovery of its XRD peaks toward the pristine positions. The fully hydrogenated film (100 °C, 1 h) demonstrates higher stability under the same conditions. Moreover, annealing the hydrogenated film in ambient atmosphere (200 °C, 1 h) drives its diffraction pattern close to the original state, confirming the reversibility of the hydrogenation process.

Supplementary References

(1) Kang, P.; Zhou, G.; Liang, J.; Ren, G.; Ji, J.; Wang, L.; Jin, C.; Xu, X. Revealing the reversal of the anomalous hall effect and the exchange bias-like effect in single-phase perpendicularly magnetized $NiCo_2O_4$ epitaxial films. *Mater. Horiz.* **2025**, *12* (11), 3762-3776, 10.1039/D4MH01764A.

(2) Chen, X.; Zhang, X.; Han, M.-G.; Zhang, L.; Zhu, Y.; Xu, X.; Hong, X. Magnetotransport Anomaly in Room-Temperature Ferrimagnetic $NiCo_2O_4$ Thin Films. *Adv. Mater.* **2019**, *31* (4), 1805260.

(3) Liu, L.; Zhou, G.; Shu, X.; Li, C.; Lin, W.; Ren, L.; Zhou, C.; Zhao, T.; Guo, R.; Xie, Q.; et al. Room-temperature spin-orbit torque switching in a manganite-based heterostructure. *Phys. Rev. B* **2022**, *105* (14), 144419.

(4) Iliev, M. N.; Silwal, P.; Loukya, B.; Datta, R.; Kim, D. H.; Todorov, N. D.; Pachauri, N.; Gupta, A. Raman studies of cation distribution and thermal stability of epitaxial spinel $NiCo_2O_4$ films. *J. Appl. Phys.* **2013**, *114* (3), 033514.

(5) Chen, H. Anomalous Hall scaling revisited in noncollinear antiferromagnets. *Newton* **2025**, *1* (3), 100100.

(6) Wang, Y.; Xu, Z.; Zhu, Y.; Liu, Q.; Hu, S.; Jiang, Y.; Chen, L. Tailoring perpendicular magnetic anisotropy and the anomalous Hall effect in epitaxial $NiCo_2O_4$ ferrimagnetic films through iron doping. *Phys. Rev. Appl.* **2025**, *24* (4), 044011.

(7) Wang, M.; Sui, X.; Wang, Y.; Juan, Y.-H.; Lyu, Y.; Peng, H.; Huang, T.; Shen, S.; Guo, C.; Zhang, J.; et al. Manipulate the Electronic and Magnetic States in $NiCo_2O_4$ Films through Electric-Field-Induced Protonation at Elevated Temperature. *Adv. Mater.* **2019**, *31* (16), 1900458.